Available online at www.sciencedirect.com
SCIENCE DIRECT®
Materials and Design 27 (2006) 976–982
Materials & Design
www.elsevier.com/locate/matdes

Three-dimensional stress analysis of rotating composite beams due to material discontinuities

M. Tahani *

Department of Mechanical Engineering, Faculty of Engineering, Ferdowsi University of Mashhad, Mashhad, Iran

Received 2 November 2004; accepted 15 February 2005
Available online 12 April 2005

Abstract

Material discontinuity could cause in-plane stress gradients that it arises out-of-plane stresses in regions of sudden transition of material properties. A layerwise laminated plate theory is adapted to laminated beams to analyze analytically the three-dimensional stress field at material discontinuities in rotating composite beams. Equations of motion are obtained by using Hamilton's principle. The beam is divided into two regions with different layups which are joined together to model the region of material discontinuity. The predicted stress distributions at the ply interfaces are shown to be in good agreement with comparative three-dimensional finite element analysis.

Keywords: Rotating composite beam; Three-dimensional stress field; Material discontinuity

1. Introduction

The problem of interlaminar stress analysis at the free edges and bonded joints of composite structures have been under investigation continuously ever since the original paper of Pipes and Pagano [1]. Numerous papers have been published on the subject over three decades. They have included, for example, the finite difference solution by Pipes and Pagano [1], the perturbation solution technique by Hsu and Herakovich [2], the finite element method by Rybicki [3] and Wang and Crossman [4], and approximate analytical solutions of Pagano [5] and Wang and Choi [6,7]. In these studies, interlaminar stresses appear at the free edges of finite composite laminates under different loading conditions have been considered. It is well known that interlaminar stresses arise in order to satisfy equilibrium at locations with in-plane stress gradients. Material discontinuity (i.e., a sudden change of material properties) within a structure is another source of arising in-plane stress gradients and, therefore, interlaminar stresses appear near the material discontinuities.

Bhat and Lagace [8] evaluated interlaminar stresses at material discontinuities using the principle of minimum complementary energy. They analyzed laminates with different layups which had been joined together. They mentioned such cases occurring at regions of implants within adaptive structures. The advent of adaptive structures has resulted in sensors made of various materials being implanted within laminated composites by cutting some plies of the laminate and placing the sensor in that location. Also a damaged region such as that caused by impact is another example of material discontinuity. Because the material properties of the impact regions are usually reduced compared to the other regions. Bhat and Lagace [8] showed that the interlaminar stresses arise in the vicinity of these material discontinuities.

Investigations of interlaminar stresses in rotating composite beams have been rare. Rotating beams are

* Tel.: +98 511 882 9538; fax: +98 511 882 9541.
E-mail address: mtahani@ferdowsi.um.ac.ir.

0261-3069/$ - see front matter
doi:10.1016/j.matdes.2005.02.009

often used as the simple model for propellers, turbine blades, and satellite booms. Hence, in this paper, it is intended to analyze three-dimensional state of stress in composite beams especially due to material discontinuities. A layerwise laminated plate theory is used to develop a layerwise laminated beam theory. The results obtained from this theory are compared with those obtained by using a finite element method. The correlation among the results indicates the theoretical approach is feasible as a conceptual design tool.

2. Theoretical formulation

It is intended here to determine the three-dimensional stress field in a rotating composite beam with uniform cross-section. Displacements of the beam are defined in a rotating rectangular Cartesian coordinate system, rigidly tied to the beam. The origin of this coordinate system is chosen to be the middle of the beam length. The x axis is the centroid axis of the undeformed beam, and y and z axes are the principal axes of the beam cross-section. It is assumed that the beam has the length $2L$ and thickness h.

Here, a layerwise laminated plate theory is developed first and then it is simplified for analysis of beam structures. It is assumed that the beam rotates with a constant angular velocity Ω (or the angular velocity is increased slowly). To this end, the problem is not time dependent.

2.1. Plate equations of motion

In this study, a layerwise laminated plate theory is used in deriving plate equations of motion. The displacement field can be represented as:

$$\begin{aligned} u_1(x,y,z) &= U_k(x,y)\Phi_k(z), \\ u_2(x,y,z) &= V_k(x,y)\Phi_k(z), \quad k = 1,2,\ldots,N+1, \\ u_3(x,y,z) &= W_k(x,y)\Phi_k(z), \end{aligned} \tag{1}$$

where for the sake of brevity, the Einstein summation convention has been introduced – a repeated index indicates summation over all values of that index. In Eq. (1) u_1, u_2 and u_3 are the displacements along the coordinate lines of a material point on the xy-plane, $U_k(x,y)$, $V_k(x,y)$, and $W_k(x,y)$ ($k = 1, 2, \ldots, N+1$) are the displacement components of all points located on the kth plane in the undeformed laminate, and $\Phi_k(z)$ are continuous functions of the thickness coordinate z (global interpolation functions). Also N denotes the total number of numerical (or mathematical) layers considered in a laminate.

It is noted that in the layerwise theory the accuracy of the displacement field in Eq. (1) depend on the shape functions $\Phi_k(z)$ and the number of surfaces in the laminate. Here, we assume that $\Phi_k(z)$ to be linear interpolation functions. On the other hand, we may increase the number of surfaces by subdividing each physical layer into a number of numerical layers. The local Lagrangian linear interpolation functions within, say, the kth layer are defined as follows (see [9,10]):

$$\phi_k^1 = \frac{z_{k+1} - z}{h_k}, \qquad \phi_k^2 = \frac{z - z_k}{h_k}, \tag{2}$$

where h_k is the thickness of the kth numerical layer and z_k denotes the z-coordinate of the bottom of the kth numerical layer. This way, the global interpolation functions $\Phi_k(z)$ may be presented as (see [9–11]):

$$\Phi_k(z) = \begin{cases} 0, & z \leqslant z_{k-1}, \\ \phi_{k-1}^2(z), & z_{k-1} \leqslant z \leqslant z_k, \quad k = 1,2,\ldots,N+1. \\ \phi_k^1(z), & z_k \leqslant z \leqslant z_{k+1}, \\ 0, & z \geqslant z_{k+1}. \end{cases} \tag{3}$$

Upon substitution of Eq. (1) into the linear strain–displacement relations of elasticity, the following results will be obtained:

$$\begin{aligned} &\varepsilon_x = \frac{\partial U_k}{\partial x}\Phi_k, \qquad \varepsilon_y = \frac{\partial V_k}{\partial y}\Phi_k, \qquad \varepsilon_z = W_k\Phi_k', \\ &\gamma_{yz} = V_k\Phi_k' + \frac{\partial W_k}{\partial y}\Phi_k, \qquad \gamma_{xz} = U_k\Phi_k' + \frac{\partial W_k}{\partial x}\Phi_k, \\ &\gamma_{xy} = \left(\frac{\partial U_k}{\partial y} + \frac{\partial V_k}{\partial x}\right)\Phi_k, \end{aligned} \tag{4}$$

with a prime indicating an ordinary derivative with respect to the independent variable z.

Using the Hamilton principle and noting that the problem is not time dependent, $3(N+1)$ equations of motion corresponding to $3(N+1)$ unknowns U_k, V_k, and W_k can be shown to be:

$$\begin{aligned} \delta U_k &: \frac{\partial M_x^k}{\partial x} + \frac{\partial M_{xy}^k}{\partial y} - Q_x^k = -\bar{I}^k\Omega^2 x - \bar{I}^{kj}U_j\Omega^2, \\ \delta V_k &: \frac{\partial M_{xy}^k}{\partial x} + \frac{\partial M_y^k}{\partial y} - Q_y^k = -\bar{I}^k\Omega^2 y - \bar{I}^{kj}V_j\Omega^2, \\ \delta W_k &: \frac{\partial R_x^k}{\partial x} + \frac{\partial R_y^k}{\partial y} - N_z^k = 0, \end{aligned} \tag{5}$$

where the generalized stress resultants are defined by:

$$\begin{aligned} (N_z^k, Q_x^k, Q_y^k) &= \int_{-h/2}^{h/2} (\sigma_z, \sigma_{xz}, \sigma_{yz})\Phi_k' \, \mathrm{d}z, \\ (M_x^k, M_y^k, M_{xy}^k, R_x^k, R_y^k) &= \int_{-h/2}^{h/2} (\sigma_x, \sigma_y, \sigma_{xy}, \sigma_{xz}, \sigma_{yz})\Phi_k \, \mathrm{d}z \end{aligned} \tag{6}$$

and the mass moments of inertia are given by:

$$(\bar{I}^k, \bar{I}^{kj}) = \int_{-h/2}^{h/2} \rho(\Phi_k, \Phi_k\Phi_j) \, \mathrm{d}z. \tag{7}$$

The boundary conditions for a laminated plate with a rectangular platform in the layerwise theory at an edge parallel to y axis involves the specification of U_k or M_x^k , V_k or M_{xy}^k and W_k or R_x^k. Similarly, at an edge parallel to x axis, the required boundary conditions can be specified.

In order to find displacement equations of motion, it is assumed that the laminate is made of orthotropic layers, with their material axes oriented arbitrarily with respect to the laminate coordinates. The linear constitutive relations for the kth orthotropic lamina with respect to the laminate coordinate axes are given by [12]:

$$\begin{Bmatrix} \sigma_x \\ \sigma_y \\ \sigma_z \\ \sigma_{yz} \\ \sigma_{xz} \\ \sigma_{xy} \end{Bmatrix}^{(k)} = \begin{bmatrix} \bar{C}_{11} & \bar{C}_{12} & \bar{C}_{13} & 0 & 0 & \bar{C}_{16} \\ \bar{C}_{12} & \bar{C}_{22} & \bar{C}_{23} & 0 & 0 & \bar{C}_{26} \\ \bar{C}_{13} & \bar{C}_{23} & \bar{C}_{33} & 0 & 0 & \bar{C}_{36} \\ 0 & 0 & 0 & \bar{C}_{44} & \bar{C}_{45} & 0 \\ 0 & 0 & 0 & \bar{C}_{45} & \bar{C}_{55} & 0 \\ \bar{C}_{16} & \bar{C}_{26} & \bar{C}_{36} & 0 & 0 & \bar{C}_{66} \end{bmatrix}^{(k)} \begin{Bmatrix} \varepsilon_x \\ \varepsilon_y \\ \varepsilon_z \\ \gamma_{yz} \\ \gamma_{xz} \\ \gamma_{xy} \end{Bmatrix}^{(k)}, \tag{8}$$

where $\bar{C}_{ij}^{(k)}$s are the transformed stiffnesses of the kth layer. Upon substitution of Eq. (4) into (8) and the subsequent results into Eq. (6) the generalized stress resultants are obtained which can be represented as follows:

$$\begin{aligned} (N_z^k, M_x^k, M_y^k, M_{xy}^k) &= (B_{13}^{jk}, D_{11}^{kj}, D_{12}^{kj}, D_{16}^{kj})\frac{\partial U_j}{\partial x} + (B_{23}^{jk}, D_{12}^{kj}, D_{22}^{kj}, D_{26}^{kj})\frac{\partial V_j}{\partial y} \\ &\quad + (A_{33}^{kj}, B_{13}^{kj}, B_{23}^{kj} B_{36}^{kj})W_j + (B_{36}^{jk}, D_{16}^{kj}, D_{26}^{kj}, D_{66}^{kj})\left(\frac{\partial V_j}{\partial x} + \frac{\partial U_j}{\partial y}\right), \\ (Q_y^k, R_y^k) &= (A_{45}^{kj}, B_{45}^{kj})U_j + (A_{44}^{kj}, B_{44}^{kj})V_j + (B_{45}^{jk}, D_{45}^{kj})\frac{\partial W_j}{\partial x} + (B_{44}^{jk}, D_{44}^{kj})\frac{\partial W_j}{\partial y}, \\ (Q_x^k, R_x^k) &= (A_{55}^{kj}, B_{55}^{kj})U_j + (A_{45}^{kj}, B_{45}^{kj})V_j + (B_{55}^{jk}, D_{55}^{kj})\frac{\partial W_j}{\partial x} + (B_{45}^{jk}, D_{45}^{kj})\frac{\partial W_j}{\partial y}, \end{aligned} \tag{9}$$

where the rigidity terms are given by:

$$\begin{aligned} A_{pq}^{kj} &= \sum_{i=1}^{N} \int_{z_i}^{z_{i+1}} \bar{C}_{pq}^{(i)} \Phi_k' \Phi_j' \, dz, \\ B_{pq}^{kj} &= \sum_{i=1}^{N} \int_{z_i}^{z_{i+1}} \bar{C}_{pq}^{(i)} \Phi_k \Phi_j' \, dz, \\ D_{pq}^{kj} &= \sum_{i=1}^{N} \int_{z_i}^{z_{i+1}} \bar{C}_{pq}^{(i)} \Phi_k \Phi_j \, dz. \end{aligned} \tag{10}$$

2.2. Beam equations of motion

Here, in this section, plate equations of motion are adapted to obtain beam equations of motion. It is assumed that all the stress resultants are functions of coordinate x only. Hence, Eq. (5) are simplified as follows:

$$\begin{aligned} \delta U_k &: \frac{\partial M_x^k}{\partial x} - Q_x^k = -\bar{I}^k \Omega^2 x - \bar{I}^{kj} U_j \Omega^2, \\ \delta V_k &: \frac{\partial M_{xy}^k}{\partial x} - Q_y^k = -\bar{I}^{kj} V_j \Omega^2, \\ \delta W_k &: \frac{\partial R_x^k}{\partial x} - N_z^k = 0. \end{aligned} \tag{11}$$

Also it is supposed that all the strains can be treated only as functions of coordinates x and z. Then Eq. (4) can be written as follows:

$$\begin{aligned} &\varepsilon_x = U_k' \Phi_k, \quad \varepsilon_y = 0, \quad \varepsilon_z = W_k \Phi_k', \\ &\gamma_{yz} = V_k \Phi_k', \quad \gamma_{xz} = U_k \Phi_k' + W_k' \Phi_k, \quad \gamma_{xy} = V_k' \Phi_k. \end{aligned} \tag{12}$$

According to Eq. (12), it is more reasonable for a beam to let M_y^k be equal to zero. Substitution of this condition into the stress resultants in Eq. (9) results in:

$$\begin{aligned} (N_z^k, M_x^k, M_{xy}^k) &= (\bar{B}_{13}^{jk}, \bar{D}_{11}^{kj}, \bar{D}_{16}^{kj})U_j' + (\bar{B}_{36}^{jk}, \bar{D}_{16}^{kj}, \bar{D}_{66}^{kj})V_j' + (\bar{A}_{33}^{kj}, \bar{B}_{13}^{kj}, \bar{B}_{36}^{kj})W_j, \\ (Q_y^k, Q_x^k, R_x^k) &= (A_{45}^{kj}, A_{55}^{kj}, B_{55}^{kj})U_j + (A_{44}^{kj}, A_{45}^{kj}, B_{55}^{kj})V_j + (B_{45}^{jk}, B_{55}^{jk}, D_{55}^{kj})W_j', \end{aligned} \tag{13}$$

where the coefficients are defined in Appendix A. Upon substitution of Eq. (13) into Eq. (11) the following governing equations of motion are obtained:

$$\begin{aligned} &\bar{D}_{11}^{kj} U_j'' - A_{55}^{kj} U_j + \bar{D}_{16}^{kj} V_j'' - A_{45}^{kj} V_j + (\bar{B}_{13}^{kj} - B_{55}^{jk}) W_j' = -\bar{I}^k \Omega^2 x - \bar{I}^{kj} U_j \Omega^2, \\ &\bar{D}_{16}^{kj} U_j'' - A_{45}^{kj} U_j + \bar{D}_{66}^{kj} V_j'' - A_{44}^{kj} V_j + (\bar{B}_{36}^{kj} - B_{45}^{jk}) W_j' = -\bar{I}^{kj} V_j \Omega^2, \\ &(B_{55}^{kj} - \bar{B}_{13}^{jk}), U_j' + (B_{45}^{kj} - \bar{B}_{36}^{jk}) V_j' + D_{55}^{kj} W_j'' - \bar{A}_{33}^{kj} W_j = 0. \end{aligned} \tag{14}$$

3. Analytical solutions

In order to obtain analytical solutions of Eq. (14), it must be noted that the numerical results indicate, however, that there exist repeated zero roots (or eigenvalues) in the characteristic equation of the set of equations in (14). To enhance the solution scheme of these equations, some small artificial terms will be added to these equations so that the characteristic roots become all distinct (see [10,11]). Therefore, Eq. (14) rewritten as follows:

$$\begin{aligned} &\bar{D}_{11}^{kj} U_j'' - A_{55}^{kj} U_j + \bar{D}_{16}^{kj} V_j'' - A_{45}^{kj} V_j + (\bar{B}_{13}^{kj} - B_{55}^{jk}) W_j' = -\bar{I}^k \Omega^2 x - \bar{I}^{kj} U_j \Omega^2 + \alpha^{kj} U_j, \\ &\bar{D}_{16}^{kj} U_j'' - A_{45}^{kj} U_j + \bar{D}_{66}^{kj} V_j'' - A_{44}^{kj} V_j + (\bar{B}_{36}^{kj} - B_{45}^{jk}) W_j' = -\bar{I}^{kj} V_j \Omega^2 + \alpha^{kj} V_j, \\ &(B_{55}^{kj} - \bar{B}_{13}^{jk}) U_j' + (B_{45}^{kj} - \bar{B}_{36}^{jk}) V_j' + D_{55}^{kj} W_j'' - \bar{A}_{33}^{kj} W_j = \alpha^{kj} W_j, \end{aligned} \tag{15}$$

where here, for convenience, α^{kj} is assumed to have the following form [10,11]:

$$\alpha^{kj} = \alpha \int_{-h/2}^{h/2} \Phi_k \Phi_j \, dz, \tag{16}$$

with α being a prescribed number such that α^{kj}s in Eq. (16) are relatively small compared to the numerical values of stiffnesses A_{55}^{kj}, A_{44}^{kj}, and $\bar{A}_{33}^{kj}$. It should be mentioned here that α^{kj} is chosen to have a form similar to the mass terms I^{kj} appearing in the equations of motion of laminated plate within Reddy's layerwise theory, with the density function ρ appearing in I^{kj} being replaced here by the small parameter α (see [9]). This way the solution of the equations in (15) will extremely be insensitive to the small number chosen for the parameter α. Next, in order to solve Eq. (15), for convenience the following state space variables are introduced:

$$\begin{aligned} &\{X_1(x)\} = \{U(x)\}, \quad \{X_2(x)\} = \{U'\} = \{X_1'\}, \\ &\{X_3(x)\} = \{V(x)\}, \quad \{X_4(x)\} = \{V'\} = \{X_3'\}, \\ &\{X_5(x)\} = \{W(x)\}, \quad \{X_6(x)\} = \{W'\} = \{X_5'\}, \end{aligned} \tag{17}$$

where for example,

$$\begin{aligned} &\{X_1\}^{\mathrm{T}} = [U_1, U_2, \ldots, U_{N+1}], \\ &\{X_2\}^{\mathrm{T}} = [U_1', U_2', \ldots, U_{N+1}'] \end{aligned} \tag{18}$$

with $\{X_3\}$ through $\{X_6\}$ being defined similarly as in (18). Substitution of Eq. (17) into Eq. (15) results in a system of $6(N+1)$ coupled first-order ordinary differential equations which may be presented as:

$$\{X'\} = [A]\{X\} + \{F\}x, \tag{19}$$

with

$$\{X\}^{\mathrm{T}} = [\{X_1\}^{\mathrm{T}}, \{X_2\}^{\mathrm{T}}, \ldots, \{X_6\}^{\mathrm{T}}]. \tag{20}$$

In Eq. (19) the coefficient matrix $[A]$ and vector $\{F\}$ are given in the Appendix A. The general solutions of Eq. (19) are given by (e.g., see [13]):

$$\{X\} = [\mathbf{U}][Q(\lambda x)]\{K\} - [A]^{-1}\{F\}x - [A]^{-2}\{F\}, \tag{21}$$

where

$$[Q(\lambda x)] = \mathrm{diag}(\mathrm{e}^{\lambda_1 x}, \mathrm{e}^{\lambda_2 x}, \ldots, \mathrm{e}^{\lambda_{6(N+1)} x}), \tag{22}$$

with $\{K\}$ being $6(N+1)$ arbitrary unknown constants of integration to be found by imposing the boundary conditions. In Eqs. (21) and (22) $[\mathbf{U}]$ and $\lambda_k (k = 1,2,\ldots,6(N+1))$ are, respectively, the matrix of eigenvectors and eigenvalues of the coefficient matrix $[A]$ which, in general, must be regarded to have complex values.

4. Results and discussion

In what follows a numerical example is presented to show that the state of stress is three-dimensional in the vicinity of the material discontinuity. It is assumed that the rotating composite beam composed of two different layups which joined together. The problem is a $[0°/90°]_s$ beam with the 90° plies replaced by the 0° plies in regions B (see Fig. 1). Thus region A is made up of a $[0°/90°]_s$ beam and regions B are made up of $[0°/0°]_s$ beams as shown in Fig. 1. Also it is assumed that the beam has the length $2L$ and thickness h, with $L = 5h$ and $a = L/2$, and is rotating with a constant angular velocity about $x = 0$ axis. In this problem, it is assumed that $\Omega = 1000$ rad/s and $h = 0.01$ m. This particular example is chosen here because interlaminar stresses arise only near the material discontinuity at the interface of regions A and B. Because of identical ply orientations in regions B no free-edge effects will be exist at $x = \pm L$. Also because the beam rotates about $x = 0$ axis and it has identical boundary conditions at $x = \pm L$, no interlaminar stresses will be arise at this point (i.e., $x = 0$).

For each regions of the beam, there exists a boundary-value problem as in Eq. (19) with the solution in Eq. (21). Therefore, there are $12(N+1)$ unknown constants of integrations for one symmetric half of the beam. In order to determine these constants, the following continuity and equilibrium conditions at the interface of regions A and B (i.e., $x = a$) must be satisfied:

$$\begin{aligned} &U_k^{(A)} = U_k^{(B)}, \quad V_k^{(A)} = V_k^{(B)}, \quad W_k^{(A)} = W_k^{(B)}, \\ &M_x^{k(A)} = M_x^{k(B)}, \quad M_{xy}^{k(A)} = M_{xy}^{k(B)}, \quad R_x^{k(A)} = R_x^{k(B)}, \end{aligned} \tag{23}$$

where the superscripts (A) and (B) show the regions A and B, respectively. In addition to the above conditions, the boundary conditions at $x = 0$ and $x = L$ must be satisfied. The boundary conditions for this problem are:

$$\begin{aligned} &U_k^{(A)} = M_{xy}^{k(A)} = R_x^{k(A)} = 0 \quad \text{at} \quad x = 0, \\ &M_x^{k(B)} = M_{xy}^{k(B)} = R_x^{k(B)} = 0 \quad \text{at} \quad x = L. \end{aligned} \tag{24}$$

The material properties of the layers are taken to be those of a T300/5208 graphite/epoxy lamina [12]:

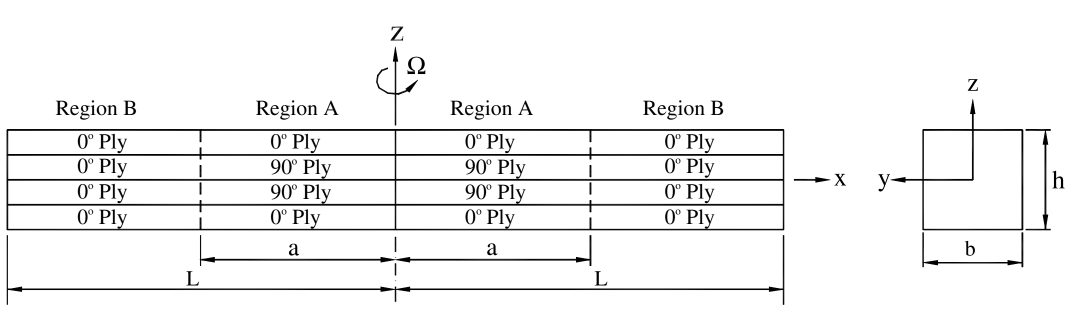

Fig. 1. The geometry of problem with a $[0°/90°]_s$ laminated beam (region A) in transition to $[0°/0°]_s$ laminated beams (regions B).

$$E_1 = 132 \text{ GPa}, \quad E_2 = E_3 = 10.8 \text{ GPa},$$
$$G_{12} = G_{13} = 5.65 \text{ GPa}, \quad G_{23} = 3.38 \text{ GPa},$$
$$\nu_{12} = \nu_{13} = 0.24, \quad \nu_{23} = 0.59, \quad \rho = 1540 \text{ kg/m}^3, \tag{25}$$

where the subscripts 1, 2, and 3 indicate the on-axis (i.e., principal) material coordinates.

To check the correctness and accuracy of the present method, the results achieved from this theory will be compared with those obtained by utilizing the commercial finite element package of ANSYS [14]. In the latter method the mesh is refined till no significant change in stress distributions is obtained. The out-of-plane stresses in the present method are determined by using Hooke's law with six numerical layers in each physical lamina (see, for example, [10,11]).

The in-plane normal stress σ_x at $z = h/4$ in 0° plies in regions A and B is shown in Fig. 2. It is noted that the stresses are taken as a small distance (of about 1/20 of the ply thickness) away from the interface for the finite element results. Also the in-plane normal stress σ_x at $z = h/4$ in 90° ply in region A and 0° ply in region B is presented in Fig. 3. It is seen that the stress distribution is discontinuous near $x = a$. It is seen in Figs. 2 and 3 that there are close agreements between the present solutions and those obtained from finite element method.

Distributions of interlaminar normal stress σ_z at $z = h/4$ along the 0°/90° interface in region A and along the 0°/0° interface in region B is displayed in Fig. 4. Also variation of interlaminar normal stress σ_z at the middle plane is shown in Fig. 5. The results show that there are sharp interlaminar stress gradients near the material discontinuity and decays away from this region as expected. The current solutions are seen to match the finite element solutions reasonably well except in the region close to the material discontinuity where the stresses have a steep gradient.

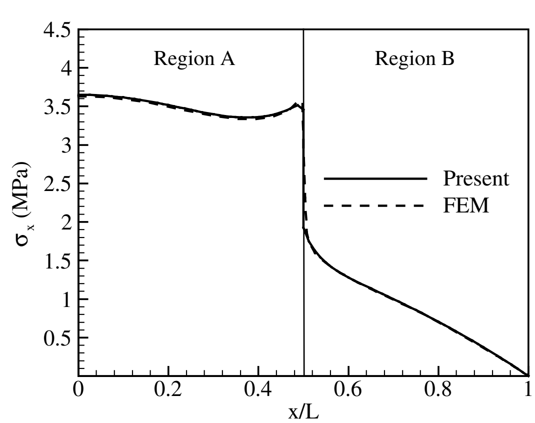

Fig. 2. Distribution of in-plane normal stress σ_x at $z = h/4$ in 0° plies in regions A and B.

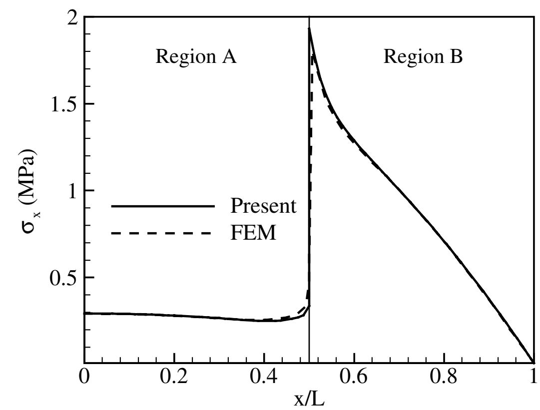

Fig. 3. Distribution of in-plane normal stress σ_x at $z = h/4$ in 90° ply in region A and 0° ply in region B.

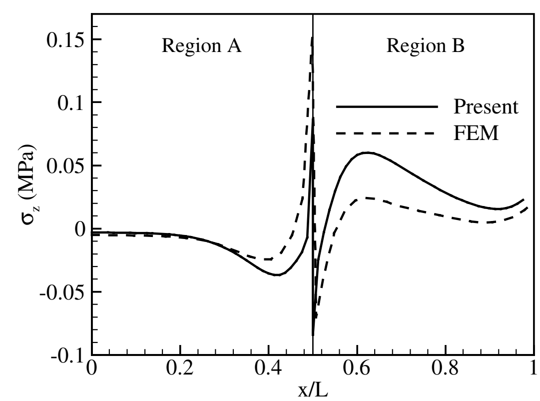

Fig. 4. Distribution of interlaminar normal stress σ_z at $z = h/4$ along the 0°/90 interface in region A and along the 0°/0° interface in region B.

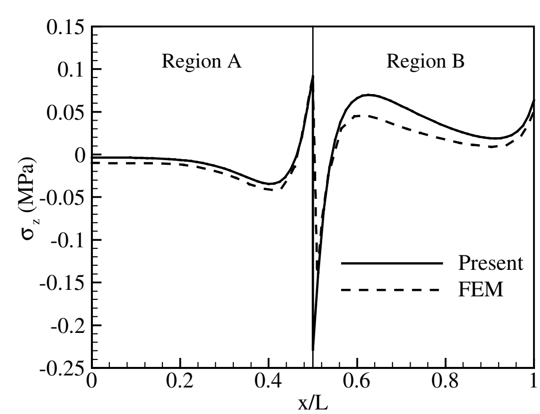

Fig. 5. Distribution of interlaminar normal stress σ_z at the middle plane.

Fig. 6 illustrates the distribution of interlaminar shear stress σ_{xz} at $z = h/4$ along the 0°/90° interface in region A and along the 0°/0° interface in region B. It is noted that σ_{xz} at the free edge ($x = L$) meet the stress free

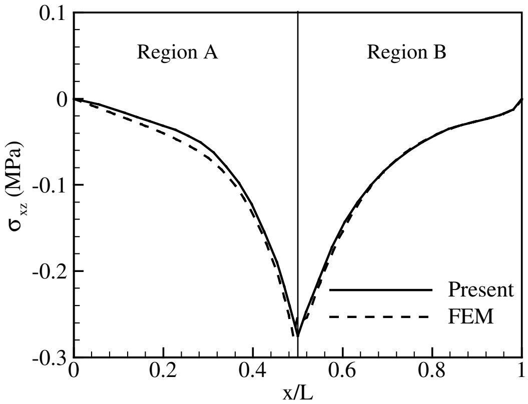

Fig. 6. Distribution of interlaminar shear stress σ_{xz} at $z = h/4$ along the 0°/90° interface in region A and along the 0°/0° interface in region B.

boundary condition with a good approximation, even though this condition has not been enforced a priori. The solution shows that the interlaminar stresses decay away from the region of the discontinuity as expected (see Figs. 4–6).

5. Conclusions

A layerwise laminated beam theory is developed by using a layerwise laminated plate theory and it is used to predict the three-dimensional stress field in the vicinity of material discontinuities in rotating composite beams with general laminations. Displacement equations of motion are obtained by using Hamilton's principle. The results obtained from this theory are compared with those obtained by a finite element method. The results indicate that there are severe out-of-plane stresses in regions near the sudden transition of material properties (material discontinuities). These stresses can initiate heterogeneous damage in the forms of delamination and transverse cracking and may cause the damage to propagate to a substantial region of the beam, resulting in a significant loss of strength and stiffness. To this end, these stresses must be considered in design of such structures.

Appendix A

The coefficients appearing in Eq. (13) are defined as:

$$[\bar{A}_{33}] = [A_{33}] - [B_{23}]^{\mathrm{T}}[D_{22}]^{-1}[B_{23}],$$

$$[\bar{B}_{13}] = [B_{13}] - [D_{12}][D_{22}]^{-1}[B_{23}],$$

$$[\bar{B}_{36}] = [B_{36}] - [D_{26}][D_{22}]^{-1}[B_{23}],$$

$$[\bar{D}_{11}] = [D_{11}] - [D_{12}][D_{22}]^{-1}[D_{12}],$$

$$[\bar{D}_{16}] = [D_{16}] - [D_{12}][D_{22}]^{-1}[D_{26}],$$

$$[\bar{D}_{66}] = [D_{66}] - [D_{26}][D_{22}]^{-1}[D_{26}].$$

The coefficient matrix $[A]$ and vector $\{F\}$ in Eq. (19) are defined as:

$$[A] = \begin{bmatrix} [0] & [I] & [0] & [0] & [0] & [0] \\ [a_1] & [0] & [a_2] & [0] & [0] & [a_3] \\ [0] & [0] & [0] & [I] & [0] & [0] \\ [b_1] & [0] & [b_2] & [0] & [0] & [b_3] \\ [0] & [0] & [0] & [0] & [0] & [I] \\ [0] & [c_1] & [0] & [c_2] & [c_3] & [0] \end{bmatrix}, \quad \{F\} = \begin{Bmatrix} \{0\} \\ \{a_4\} \\ \{0\} \\ \{b_4\} \\ \{0\} \\ \{0\} \end{Bmatrix}$$

where $[0]$ and $[I]$ are $(N+1)\times(N+1)$ square zero and identity matrices, respectively, and $\{0\}$ is a zero vector with $N+1$ rows. The remaining matrices and vectors in the above equations are as follows:

$$[a_1] = [d_1]^{-1}[d_2],$$

$$[a_2] = [d_1]^{-1}[d_3],$$

$$[a_3] = [d_1]^{-1}[d_4],$$

$$\{a_4\} = [d_1]^{-1}\{d_5\},$$

$$[b_1] = [\bar{D}_{66}]^{-1}([A_{45}] - [\bar{D}_{16}][a_1]),$$

$$[b_2] = [\bar{D}_{66}]^{-1}([A_{44}] - [\bar{D}_{16}][a_2] - [\bar{I}]\Omega^2 + [\alpha]),$$

$$[b_3] = [\bar{D}_{66}]^{-1}([B_{45}]^{\mathrm{T}} - [\bar{B}_{36}] - [\bar{D}_{16}][a_3]),$$

$$\{b_4\} = -[\bar{D}_{66}]^{-1}[\bar{D}_{16}]\{a_4\},$$

$$[c_1] = [D_{55}]^{-1}([\bar{B}_{13}]^{\mathrm{T}} - [B_{55}]),$$

$$[c_2] = [D_{55}]^{-1}([\bar{B}_{36}]^{\mathrm{T}} - [B_{45}]),$$

$$[c_3] = [D_{55}]^{-1}([\bar{A}_{33}] + [\alpha]),$$

with

$$[d_1] = [\bar{D}_{11}] - [\bar{D}_{16}][\bar{D}_{66}]^{-1}[\bar{D}_{16}],$$

$$[d_2] = [A_{55}] - [\bar{D}_{16}][\bar{D}_{66}]^{-1}[A_{45}] - [\bar{I}]\Omega^2 + [\alpha],$$

$$[d_3] = [A_{45}] - [\bar{D}_{16}][\bar{D}_{66}]^{-1}([A_{44}] - [\bar{I}]\Omega^2 + [\alpha]),$$

$$[d_4] = [B_{55}]^{\mathrm{T}} - [\bar{B}_{13}] + [\bar{D}_{16}][\bar{D}_{66}]^{-1}([\bar{B}_{36}] - [B_{45}]^{\mathrm{T}}),$$

$$\{d_5\} = -\{\bar{I}\}\Omega^2,$$

$[\bar{I}]$ and $\{\bar{I}\}$ are the matrix and vector of mass moments of inertia defined in Eq. (7).

References

[1] Pipes RB, Pagano NJ. Interlaminar stresses in composite laminates under uniform axial extension. J Compos Mater 1970;4:538–48.

[2] Hsu PW, Herakovich CT. Edge effects in angle-ply composite laminates. J Compos Mater 1977;11:422–8.

[3] Rybicki EF. Approximate three-dimensional solutions for symmetric laminates under inplane loading. J Compos Mater 1971;5:354–60.

[4] Wang ASD, Crossman FW. Some new results on edge effect in symmetric composite laminates. J Compos Mater 1977;11:92–106.

[5] Pagano NJ. Free edge stress fields in composite laminates. Int J Solids Struct 1978;14:401–6.

[6] Wang SS, Choi I. Boundary-layer effects in composite laminates: Part 2 – free-edge stress solutions and basic characteristics. J Appl Mech 1982;49:549–60.

[7] Wang SS, Choi I. Boundary-layer effects in composite laminates: Part 1 – free-edge stress singularities. J Appl Mech 1982;49:541–8.

[8] Bhat NV, Lagace PA. An analytical method for the evaluation of interlaminar stresses due to material discontinuities. J Compos Mater 1994;28(3):190–210.

[9] Nosier A, Kapania RK, Reddy JN. Free vibration analysis of laminated plates using a layerwise theory. AIAA J 1993;13(12):2335–46.

[10] Tahani M, Nosier A. Three-dimensional interlaminar stress analysis at free edges of general cross-ply composite laminates. Mater Des 2003;24:121–30.

[11] Tahani M, Nosier A. Accurate determination of interlaminar stresses in general cross-ply laminates. Mech Adv Mater Struct 2004;11(1):67–92.

[12] Herakovich CT. Mechanics of fibrous composites. New York: John Wiley; 1998.

[13] Gopal M. Modern control system theory. 2nd ed. New Age International (P) Limited; 1993.

[14] ANSYS, Release 5.4 UP19970828, SAS IP, Inc., 1997.